Inorg. Chem. **2006**, *45*, 7083–7090

Interaction of Vanadyl (VO^{2+}) with Ligands Containing Serine, Tyrosine, and Threonine

Martin Ebel and Dieter Rehder*

Department of Chemistry, University of Hamburg, D-20146 Hamburg, Germany

Received February 21, 2006

Reaction of vanadyl sulfate with an aldehyde (2-hydroxy-1-naphthaldehyde (nap); 3-methoxysalicylaldehyde = *o*-vanillin (van)) and an amino acid carrying an OH group (L-tyrosine (L-Tyr); L-serine (L-Ser), L-threonine (L-Thr)) yielded the complexes [VO(nap-D-Tyr)(H_2O)] **1a**, [VO(van-D,L-Tyr)(H_2O)] **1c**, [VO(nap-Ser)(H_2O)] **2a**, [VO(van-D,L-Ser)(H_2O)] **2b**, [VO(nap-Thr)(H_2O)] **3a**, and [VO(van-Thr)(H_2O)] **3b**. [VO(nap-L-Tyr(H_2O)], **1b**, was obtained from the reaction between [VO(nap)$_2$] and L-TyrOMe. The crystal and molecular structures of **1a**·CH_3OH, **1b**·CH_3OH, **1c**·H_2O, **2b**·2H_2O, and the Schiff base nap-D,L-TyrOMe (**4**) are reported. The ligands coordinate in a tridentate manner through the phenolate component of nap or van, the imine nitrogen, and the carboxylate of the amino acid. Direct coordination of the (deprotonated) OH amino acid functionality is not observed in these complexes. Instead, the OH groups are involved in hydrogen bonding, leading, along with π–π stacking, to extended one- and three-dimensional supramolecular networks. The relevance for the interaction between oxovanadium(IV,V) and proteins having serine, threonine, or tyrosine at their reactive sites is addressed.

Introduction

The interaction of vanadates (V) and vanadyl (VO^{2+}) with OH-functional amino acid side chains in proteins, commonly enzymes, can modify, deactivate, or activate the enzyme. An example of deactivation is the vanadate-dependent photooxidation of serine to formylglycine (and further to formiate) in the myosin subfragment S1,[1,2] or the vanadate-dependent inactivation, on irradiation, of ribulose-1,5-diphosphate carboxylase/oxygenase.[3] In both cases, inactivation is succeeded by cleavage of the protein. A corresponding initial photooxidation of active site threonine and serine by vanadate and decavanadate, respectively, followed by photocleavage has been reported for sarcoplasmatic reticulum ATPase.[4] The importance of the presence of threonine in the TGES sequence of domain A of the Na,K-ATPase for inhibition by vanadate has been demonstrated.[5] Reactions related to activation are the light-induced, oxidative activation of the C91S mutant of arylsulfatase-B[6] and serine-sulfhydrase[7] by conversion of cysteine to serine accomplished by vanadate. In these reactions, vanadate is supposed to be in direct contact with serine (or threonine), which can be achieved by either hydrogen bonds, formation of a vanadate ester such as $HVO_3(OSer)^-$,[8,9] or by direct coordination of serine or serinate into a fifth position, forming a frozen-in trigonal-bipyramidal "transition-state intermediate", as evidenced by X-ray diffraction analysis of the vanadate-inhibited *E. coli* alkaline phosphatase.[10]

In all of these light-induced, vanadate-dependent reactions, vanadate is the primary electron acceptor and thus reduced to vanadyl, which is supposed to remain close to the active site because it can be expected to effectively coordinate to a multifunctional O- and N-environment provided by the amino acid and modified amino acid constituents of the protein;[11] is also plays an important secondary role, as it can promote the generation of superoxide and hydroxyl radicals.[12]

* To whom correspondence should be addressed. E-mail: rehder@chemie.uni-hamburg.de.

(1) (a) Grammer, J. C.; Loo, J. A.; Edmonds, C. G.; Cremo, C. R.; Yount, R. G. *Biochemistry* **1996**, *35*, 15582−15592. (b) Cremo, C. R.; Long, G. T.; Grammer, J. C. *Biochemistry* **1990**, *29*, 7982−7990.
(2) Mulrad, A.; Peyser, Y. M.; Ringel, I. *Eur. J. Biochem.* **1991**, *201*, 405−415.
(3) Mogel, S. N.; McFadden, B. A. *Biochemistry* **1989**, *28*, 5428−5431.
(4) Hua, S.; Inesi, G.; Toyoshima, C. *J. Biol. Chem.* **2000**, *275*, 30546−30550.
(5) Toustrup-Jensen, M.; Vilsen, B. *J. Biol. Chem.* **2003**, *278*, 11402−11410.
(6) Christianson, T. M.; Starr, C. M.; Zankel, T. C. *Biochem. J.* **2004**, *382*, 581−587.
(7) Meisch, H. U.; Kappesser, S. *Biochim. Biophys. Acta* **1987**, *925*, 234−237.
(8) Rehder, D. *Inorg. Chem.* **1988**, *27*, 4312−4316.
(9) Gorzsás, A.; Andersson, I.; Schmidt, H.; Rehder, D.; Pettersson, L. *Dalton Trans.* **2003**, 1161−1167.
(10) Holtz, K. M.; Stec, B.; Kantrowitz, E. R. *J. Biol. Chem.* **1999**, *274*, 8351−8354.

10.1021/ic0602953 CCC: $33.50
Published on Web 08/03/2006

Further, V^{IV} is present as vanadate(IV), $VO(OH)_3^-$, at nanomolar concentrations in the pH range 6−8,[13] and may, similarly to vanadate(V) ($H_2VO_4^- \equiv VO_2(OH)_2^-$), act as a phosphate analogue.

As far as tyrosine is concerned, the binding of vanadyl and vanadate to the tyrosine residues in the C- and N-terminal ends of transferrin is well-established,[11a,14] as is the direct binding of vanadate to tyrosine in tyrosyl−DNA−phosphodiesterase.[15] Tyrosine itself interacts rather ineffectively with vanadate; the formation constants K_f for the formation of $HVO_3(OTyr)^-$ amounts to 1.8 M^{-1}.[16] Dipeptides containing tyrosine are more effective binders (K_f = 128 M^{-1} for Gly-Tyr[17]), although the main complexes formed with VO^{3+} and VO^{2+} exclude tyrosine from direct binding.[18−20] In this respect, i.e., leaving the OH function uncoordinated, dipeptides containing serine behave accordingly.[21,22] In the structurally characterized complexes [$VO(NH_2O)$Ser][23] and [VO-(His-en-Tyr)] (en = ethylenediamine),[24] the OH again remains uncoordinated. An additional implication is the redox lability of vanadate in the presence of peptides with tyrosine residues.[19]

In the present work, we investigate the interaction between vanadyl and ligands containing the amino acid moieties tyrosine, serine, or threonine. Because amino acids and oligopeptides do not efficiently coordinate to vanadyl in the absence of auxiliary ligands (such as *o*-phenanthroline[25]), we have employed the amino acids as Schiff base derivatives, using *o*-hydroxynaphthadehyde (nap) or *o*-vanillin (van) as the carbonyl component and thus providing strong ligating properties. Preliminary results on some of these complexes have been published previously.[26] Structurally characterized Schiff base complexes containing amino acids without a function in the side chain include [VO(sal-Ala)H_2O],[27] [VO-(sal-Gly)py_2] (sal = salicylidene, py = pyridine),[28a] and the dinuclear oxovanadium(V) complex [V_2O_3(sal-val)$_2H_2O$].[28b] A dinuclear oxovanadium(IV,V) complex containing serine, such as $[V_2O_3(\text{sal-Ser})_2]^-$, has been reported by Costa Pessoa.[22]

Experimental Section

Materials and Methods. The following starting materials were obtained from commercial sources (Sigma, Fluka) and used without further purification: L-tyrosine (L-Tyr), L-tyrosine methylester, L-serine (L-Ser), L-threonine (L-Thr), 2-hydroxy-1-naphthaldehyde (nap), *o*-vanillin (van), and vanadyl sulfate pentahydrate ($VOSO_4 \cdot 5H_2O$). Solvents (water, methanol, ethanol, THF, diethyl ether, and pentane) were degassed and saturated with nitrogen. All operations were performed under nitrogen (Schlenk technique) in order to prevent the oxidation of V^{IV} to V^V in solution. The isolated and dried (under vacuum at room temperature) complexes are air-stable.

Elemental analyses were carried out with a Heraeus CHN−O rapid analyzer. IR spectra were obtained in KBr pellets on a Perkin−Elmer FT-IR spectrometer 1720XFT, solution UV−vis spectra in glass cuvettes with a Varian Cary 5E spectrometer, and circular dichroism (CD) spectra on a spectropolarimeter Jasco J500C. EPR spectra were scanned at room temperature and 100(2) K (1−5 mM aqueous or methanolic solution) in 4 mm diameter capillaries on a Bruker EPR-300E instrument in the range 9.42−9.74 GHz. Parameter adaption was carried out with the Bruker program system WINEPR SimFonia, version 1.25. For the collection of FAB mass spectral data, a VG analytical mass spectrometer 70-250S, equipped with a xenon source, was employed. *m*-Nitrobenzyl alcohol was used as a matrix. Selected IR data and FAB-MS molecular peaks are included in the section on the preparation of complexes; UV−vis and EPR data are collated in the tables.

Data collections for single-crystal structure determinations were carried out at 153(2) K with an Enraf−Nonius CAD4 four-circle diffractometer (graphite monochromator, Cu Kα irradiation; **2b**) or with a Bruker SMART CCD diffractometer (graphite monochromator, Mo Kα irradiation; **1a**−**c**, **4**). Frames were read out with the program SAINT; absorption corrections were carried out with SADABS. The program XPREP was used for the determination of the space group. The program systems SHELXS-97 and SHELXL-97 were employed for phase problems and structure refinement. Hydrogen atoms not participating in hydrogen bonds were placed into calculated positions, other hydrogens were located in the Fourier map. For structure and refinement data, see Table 1. CCDC numbers: **1a**·CH_3OH, 206712; **1b**·CH_3OH, 235864; **1c**·H_2O, 235866; **2b**·$2H_2O$, 235867; nap-D,L-TyrOMe (**4**), 235865.

Preparation of Complexes. [VO(nap-D-Tyr)(H_2O)]·CH_3OH, 1a·CH_3OH. L-Tyrosine (450 mg, 2.5 mmol), 2-hydroxy-1-naphthaldehyde (450 mg, 2.6 mmol), vanadyl sulfate pentahydrate (630 mg, 2.5 mmol), and sodiumacetate trihydrate (0750 mg, 5.5 mmol) were dissolved in a mixture of 25 mL of water and 10 mL of

(11) (a) Smith, C. A.; Ainscough, E. W.; Brodie, A. M. *J. Chem Soc. Dalton Trans*. **1995**, 1121−1126. (b) Gerfen, G. J.; Hanna, P. M.; Chastee, N. D.; Singel, D. J. *J. Am. Chem. Soc.* **1991**, *113*, 9513−9519. (c) Zhang, C.; Markham, G. D.; LoBrutto, R. *Biochemistry* **1993**, *32*, 9866−9873. (d) Bogumil, R.; Hüttermann, J.; Kappl, R.; Stabler, R.; Sudfeldt, C.; Witzel, H. *Eur. J. Biochem*. **1991**, *196*, 305−312. (e) de Boer, E.; Boon, K.; Wever, R. *Biochemistry* **1988**, *27*, 1629−1635.

(12) (a) Shi, X.; Dalal, N. S. *Arch. Biochem. Biophys*. **1993**, *307*, 336−341. (b) Liochev, S.; Fridovich, I. *Arch. Biochem. Biophys*. **1987**, *255*, 274−278. (c) Carmichael, A. J. *FEBS Lett*. **1990**, *261*, 165−170.

(13) (a) Crans, D. C.; Smee, J. J.; Gaidamauskas, E.; Yang, L. *Chem. Rev*. **2004**, *104*, 849−902. (b) Ianuzzi, M. M.; Rieger, P. H. *Inorg. Chem*. **1975**, *14*, 2895−2899.

(14) (a) Butler, A.; Eckert, H. *J. Am. Chem. Soc*. **1989**, *111*, 2802−2809. (b) Chasteen, N. D.; Lord, E. M.; Thompson, H. J.; Grady, J. K. *Biochim. Biophys. Acta* **1986**, *884*, 84−92.

(15) (a) Davies, D. R.; Interthal, H.; Champoux, J. J.; Hol, W. G. J. *J. Med. Chem*. **2004**, *47*, 829−837. (b) Davies, D. R.; Interthal, H.; Champoux, J. J.; Hol, W. G. J. *Chem. Biol*. **2003**, *10*, 139−147.

(16) Galeffi, B.; Tracey, A. S. *Can. J. Chem*. **1988**, *66*, 2565−2569.

(17) Rehder, D.; Holst, H.; Priebsch, W.; Vilter, H. *J. Inorg. Biochem*. **1991**, *41*, 171−185.

(18) Tracey, A. S.; Jaswal, J. S.; Nxumalo, F.; Angus-Dunne, S. J. *Can. J. Chem*. **1995**, *73*, 489−498.

(19) Crans, D. C.; Holst, H.; Keramidas, A.; Rehder, D. *Inorg. Chem*. **1995**, *34*, 2524−2534.

(20) Tasiopoulos, A. J.; Deligiannakis, Y. G.; Woolins, J. D.; Slawin, A. M. Z.; Kabanos, T. A. *Chem. Commun*. **1998**, 569−570.

(21) Grüning, C.; Rehder, D. *J. Inorg. Biochem*. **2000**, *80*, 185−189.

(22) Costa Pessoa, J.; Silva, J. A. L.; Vieira, A. L.; Vilas-Boas, L.; O'Brien, P.; Thornton, P. *J. Chem. Soc., Dalton Trans*. **1992**, 1745−1749.

(23) Keramidas, A.; Miller, S. M.; Anderson, O. P.; Crans, D. C. *J. Am. Chem. Soc*. **1997**, *119*, 8901−8915.

(24) Kawabe, K.; Suekuni, T.; Inada, T.; Yamamoto, K.; Tadokoro, M.; Kojima, Y.; Fijisawa, Y.; Sakurai, H. *Chem. Lett*. **1998**, 1155−1156.

(25) Tasiopoulos, A. J.; Vlahos, A. T.; Keramidas, A. D.; Kabanos, T. A.; Deligiannakis, Y. G.; Raptopoulou, C. P.; Terzis, A. *Angew. Chem., Int. Ed*. **1996**, *35*, 2531−2533.

(26) (a) Ebel, M.; Rehder, D. *Inorg. Chim. Acta* **2003**, *356*, 210−214. (b) Rehder, D.; Ebel, M.; Wikete, C.; Santoni, G.; Gätjens, J. *Pure Appl. Chem*. **2005**, *77*, 1607−1616.

(27) Hämäläinen, A. R.; Turpeinen, U.; Ahlgrén, M. *Acta Crystallogr., Sect. C* **1985**, *41*, 1726.

(28) (a) Cavaco, I.; Costa Pessoa, J.; Costa, D.; Duarte, M. I.; Gillard, R. D.; Matias, P. *J. Chem. Soc., Dalton Trans*. **1994**, 149−157. (b) Cavaco, I.; Costa Pessoa, J.; Duarte, M. T.; Henriques, R. T.; Matias, P. M.; Gillard, R. D. *J. Chem. Soc., Dalton Trans*. **1996**, 1989−1996.

Table 1. Crystal and Structure Refinement Data

	1a·CH_3OH	**1b**·CH_3OH	**1c**·H_2O	**2b**·$2H_2O$	**4**
empirical formula	$C_{21}H_{21}NO_7V$	$C_{21}H_{21}NO_7V$	$C_{17}H_{19}NO_8V$	$C_{11}H_{17}NO_9V$	$C_{12}H_{19}NO_4$
molecular mass (g/mol)	450.33	450.33	416.27	358.20	349.37
space group	$P2_12_12_1$	$P2_12_12_1$	$P2_1/n$	$P\bar{1}$	$P2_1/n$
a (Å)	7.2613(3)	7.2537(11)	8.4513(7)	8.7061(18)	8.6949(4)
b (Å)	12.6250(6)	12.6051(19)	14.6731(13)	9.278(2)	10.8809(6)
c (Å)	21.9597(10)	21.924(3)	14.4877(13)	9.311(2)	18.3954(9)
α (deg)				80.712(2)	
β (deg)			105.482(2)	84.127(3)	94.5310(10)
γ (°)				84.078(3)	
V (Å^3)	2013.13(16)	2004.6(5)	1731.4(3)	735.5(3)	1734.92(15)
Z	4	4	4	2	4
D_{calcd} (g/mL)	1.486	1.492	1.597	1.617	1.338
μ (mm^{-1})	0.537	0.539	0.621	0.720	0.093
F(000)	932	932	860	370	736
cryst size (mm^3)	0.6 × 0.1 × 0.1	0.4 × 0.24 × 0.1	0.4 × 0.24 × 0.12	0.8 × 0.12 × 0.07	0.9 × 0.3 × 0.3
no. of reflns	50712	23827	20146	8054	46705
data/restraints/params	5846/0/292	4570/5/284	3787/6/261	3019/10/222	6276/0/261
R1 ($I < 2\sigma(I)$)	0.0439	0.0451	0.0408	0.0646	0.0527
w*R*2 ($I < 2\sigma(I)$)	0.0882	0.1000	0.0804	0.1488	0.1498
R1 values (all data)	0.0685	0.0510	0.0601	0.0840	0.0623
wR2 (all data)	0.1178	0.1026	0.0849	0.1574	0.1573
Flack param	0.00(3)	0.01(2)			
excess electron density max/min (e Å^{-3})	0.707/−0.518	0.878/−0.391	0.481/−0.281	0.733/−0.706	0.436/−0.224

methanol to yield a brown solution and a beige precipitate. This mixture was refluxed overnight. The color changed to light green and finally to a light brown-green. The green-brown precipitate was filtered off, and the filtrate was allowed to stand at room temperature for 3 days to yield dark green crystals suitable for X-ray diffraction analyses. The polycrystalline precipitate was washed twice with 25 mL of water and once with 10 mL of toluene and then dried. This raw material was redissolved in 80 mL of methanol and reprecipitated with 100 mL of water, filtered off, and dried. Overall yield: 780 mg (1.7 mmol, 68%). Whereas the crystals contain the tyrosine moiety in the D-configuration, the bulk material is a racemate, with L-tyrosine outweighing D-tyrosine (CD evidence; see Discussion). Elemental anal. Calcd for $C_{21}H_{21}NO_7V$: C, 56.01; H, 4.70; N, 3.11. Found: C, 56.16; H, 4.65; N, 3.06. IR (cm^{-1}): 3398 (*ν* OH), 3204 (*ν* OH [H_2O]), 1660 (ν_{as} COO^-), 1621 and 1609 (C═N), 1391 (ν_s COO^-), 1361 (*δ* OH), 1246 and 1106 (*ν* CO), 988 and 976 (*ν* V═O). FAB-MS: 401 $(M + H)^+$, 801 $(2M + H)^+$.

[VO(nap)$_2$] and [VO(nap-L-Tyr)(H$_2$O)]·CH$_3$OH, 1b·CH$_3$OH. 2-Hydroxy-1-naphthaldehyde (8.6 g, 0.05 mol), $VOSO_4·5H_2O$ (6.32 g, 0.025 mol), and sodiumacetate trihydrate (6.8 g, 0.05 mol) were dissolved in water (45 mL) and ethanol (40 mL) and stirred for 4 h at room temperature. The light green precipitate was filtered off, washed twice with 10 mL of ethanol and twice with 10 mL of diethyl ether, and dried to form [VO(nap)$_2$]·H_2O. Yield: 70%. Elemental anal. Calcd for $C_{22}H_{14}O_5V·H_2O$: C, 61.84; H, 3.77. Found: C, 61.56; H, 3.75. IR (cm^{-1}): 3401 (*ν* OH [H_2O]), 3069 and 2921 (*ν* CH), 1618 (*ν* C═O), 1600, 1582 and 1540 (*ν* C═C arom.), 1468 and 1455 (*δ* CH_2), 1386 and 1195 (*ν* CO), 979 (*ν* V═O), 831 and 746 (*δ* CH). FAB-MS: 401 $(M + H)^+$, 801 $(2M + H)^+$.

[VO(nap)$_2$]·H_2O (427 mg, 1 mmol), L-tyrosine-methylester (195 mg, 1 mmol), and sodiumacetate trihydrate (136 mg, 1 mmol) were dissolved in 20 mL of methanol and 10 mL of water and refluxed for 2 h. The dark green solution was separated from unreacted [VO(nap)$_2$] by filtration. Dark green crystals of **1b**·CH_3OH were recovered from the filtrate after 3 days at room temperature. Elemental anal. Calcd for $C_{21}H_{21}NO_7V$: C, 56.01; H, 4.70; N, 3.11. Found: C, 56.00; H, 4.67; N, 3.01. The IR pattern is similar to that of **1a**.

[VO(van-D,L-Tyr)(H$_2$O)]·H$_2$O, 1c·H$_2$O. L-Tyrosine (450 mg, 2.5 mmol), *o*-vanillin (380 mg, 2.5 mmol), $VOSO_4·5H_2O$ (630 mg, 2.5 mmol), and sodiumacetate trihydrate (750 mg, 5.5 mmol) were dissolved in water (10 mL) and methanol (25 mL) and refluxed. After the solution was cooled back to room temperature, the dark green residue was extracted with several portions of THF, and the THF extracts were concentrated to half of the original volume. The addition of pentane yielded a green solid, which was filtered off, washed with pentane, and dried. According to elemental analysis, the composition corresponds to **1c**·H_2O·0.75THF + 1/8 mole of admixed Na_2SO_4. Yield: 680 mg (1.45 mmol, 58%). Crystals of **1c**·H_2O were obtained by layering a dilute THF solution of **1c** with pentane under an inert gas atmosphere. Suitable crystals grew at the interface within several weeks at room temperature. Elemental analysis for the bulk material, calcd for $C_{21}H_{21}NO_7V·3/4THF·1/8Na_2SO_4$; C, 51.10; H, 4.93; N, 2.98. Found: C, 51.1; H, 4.9; N, 2.9. IR (cm^{-1}): 3435 (*ν* OH), 3260 (*ν* OH [H_2O]), 1660 (ν_{as} COO^-), 1630 and 1605 (C═N), 1404 (ν_s COO^-), 1363 (*δ* OH), 1250 and 1084 (*ν* CO), 990 (*ν* V═O). FAB-MS: 381 $(M + H)^+$, 783 $(2M + Na)^+$.

[VO(nap-D,L-Ser)(H$_2$O)], 2a. L-Serine (105 mg, 1 mmol), 2-hydroxy-1-naphthaldehyde (177 mg, 1.03 mmol), $VOSO_4·5H_2O$ (253 mg, 1 mmol), and sodiumacetate trihydrate (275 mg, 2 mmol) dissolved in methanol (20 mL) and water (10 mL) were refluxed for 2 h. An intermediately formed green precipitate redissolved. The warm reaction mixture was evaporated to dryness. THF (25 mL) was added to the green-black residue and refluxed for 1.5 h; while it was still hot, the solution was separated from a white residue by filtration. The green filtrate was allowed to cool to room temperature and treated with 35 mL of pentane. The dark green solid was filtered off, washed with pentane, and dried. Yield: 260 mg (0.72 mmol, 72%). According to the elemental analysis, the compound contains impurities of sodium sulfate and hydroxynaphthaldehyde. Elemental anal. Calcd for $C_{14}H_{13}NO_6V·1/12Na_2SO_4·1/24C_{11}H_8O_2$: C, 48.08; H, 3.72; N, 3.88; S, 0.74. Found; C, 48.12; H, 3.72; N, 3.82; S, 0.74. IR (cm^{-1}): 3429 (*ν* OH), 3250 (*ν* OH [H_2O]), 1657 (ν_{as} COO^-), 1621 and 1606 (C═N), 1392 (ν_s COO^-), 1361 and 1342 (*δ* OH), 1250 and 1063 (*ν* CO), 984 (*ν* V═O). FAB-MS: 325 $(M + H)^+$, 347 $(M + Na)^+$, 649 $(2M + H)^+$, 671 $(2M + Na)^+$.

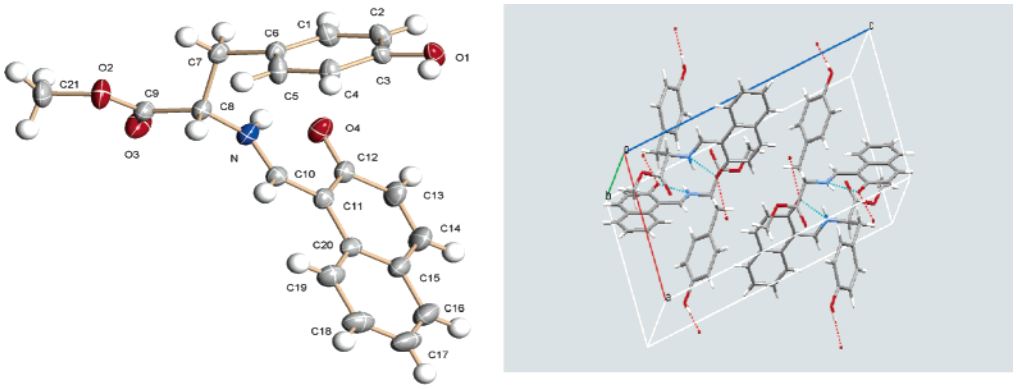

Figure 1. Molecular structure (left) of one of the molecules (L-enantiomer) in the unit cell, and packing diagram (right) of the racemic Schiff base **4** (hydrogen bonds are indicated by dotted lines in blue (intramolecular) and red (intermolecular).

[VO(van-D,L-Ser)(H$_2$O)], 2b, and [VO(van-D,L-Ser)(H$_2$O)]·2H$_2$O, 2b·2H$_2$O. The preparation was carried out as described for **2a**, substituting the naphthaldehyde for *o*-vanillin (152 mg, 1 mmol). The THF extract was layered with pentane and allowed to stand at 4 °C for several weeks. Dark green crystals of **2b**·2H$_2$O suitable for an X-ray structure analysis were obtained, along with a nonuniform precipitate. This was extracted with 75 mL of boiling THF; the THF extract was reduced to 25 mL by evaporation in vacuo and treated with 75 mL of pentane. The dark green solid was filtered off, washed with pentane, and dried to yield 160 mg (0.48 mmol, 48%) of dark green **2b**·1/8THF. Elemental anal. Calcd for C$_{11}$H$_{13}$NO$_7$V·1/8THF: C, 41.71; H, 4.26; N, 4.26. Found: C, 41.57; H, 4.33; N, 4.29. IR (cm^{-1}): 3458 (ν OH), 3252 (ν OH [H$_2$O]), 1685 (ν_{as} COO$^-$), 1623 and 1605 (C=N), 1414 (ν_s COO$^-$), 1330 and 1390 (δ OH), 1254 and 1072 (ν CO), 988 (ν V=O).

[VO(nap-D,L-Thr)(H$_2$O)], 3a. L-Threonine (300 mg, 2.5 mmol), 2-hydroxy-1-naphthaldehyde (450 mg, 2.6 mmol), VOSO$_4$·5H$_2$O (640 mg, 2.5 mmol), and sodiumacetate trihydrate (750 mg, 5.5 mmol) were dissolved in 25 mL of methanol and refluxed for 30 min. The originally dark green reaction mixture turned brownish after a couple of minutes, but regained the green color after being cooled back to room temperature. After 2 days at room temperature, a light green precipitate (Na$_2$SO$_4$) had formed, which was removed by filtration. The filtrate was evaporated to dryness; the residue was dissolved in 20 mL of THF and treated with 60 mL of pentane. The dark brown solid thus obtained was redissolved in THF, filtered, and reprecipitated with pentane to yield a greenish brown solid, which was filtered off and dried. Yield: 220 mg (0.59 mmol, 59%). Elemental anal. Calcd for C$_{15}$H$_{15}$NO$_6$V·1/4THF: C, 51.35; H, 4.58; N, 3.74. Found: C, 51.59; H, 4.45; N, 3.68. IR (cm^{-1}): 3431 (ν OH), ~3250 (sh, ν OH [H$_2$O]), 1650 (ν_{as} COO$^-$), 1620 and 1605 (C=N), 1391 (ν_s COO$^-$), 1362 and 1341 (δ OH), 1250 and 1098 (ν CO), 985 and 977 (ν V=O). FAB-MS: 339 (M + H)$^+$, 361 (M + Na)$^+$, 677 (2M + H)$^+$, 699 (2M + Na)$^+$.

[VO(van-D,L-Thr)(H$_2$O)], 3b. L-Threonine (300 mg, 2.5 mmol), *o*-vanillin (380 mg, 2.5 mmol), VOSO$_4$·5H$_2$O (640 mg, 2.5 mmol), and sodiumacetate trihydrate (750 mg, 5.5 mmol) dissolved in 15 mL of methanol were refluxed overnight. The green reaction mixture was cooled back to room temperature, allowed to stand for 2 h, and separated from a beige precipitate by filtration. The filtrate was evaporated to dryness, treated with THF, and stored at 4 °C overnight to yield a green-black solid. To the filtrate was added pentane to produce additional precipitate. The combined precipitates were washed with pentane, dried, and recrystallized from THF/pentane. Yield: 610 mg (1.77 mmol, 71%). Elemental anal. Calcd for C$_{12}$H$_{15}$NO$_7$V·1/8THF: C, 43.49; H, 4.67; N, 4.06. Found: C, 43.61; H, 4.52; N, 3.91. IR (cm^{-1}): 3435 (ν OH), ~3250 (sh, ν OH [H$_2$O]), 1652 (ν_{as} COO$^-$), 1626 and 1604 (C=N), 1399 (ν_s COO$^-$), 1305 (δ OH), 1250 and 1083 (ν CO), 983 (ν V=O). FAB-MS: 319 (M + H)$^+$, 637 (2M + H)$^+$, 659 (2M + Na)$^+$.

***N*-(2-Oxinaphthalidene)-D,L-tyrosinemethylester, Nap-D,L-Tyr-OMe, 4.** L-Tyrosine methylester (390 mg, 2 mmol) and 2-hydroxy-1-naphthaldehyde (360 mg, 2.3 mmol) were refluxed for 45 min in 25 mL of methanol to yield a yellow precipitate. The reaction mixture was kept at −20 °C overnight; the yellow precipitate was filtered off, washed with a small amount of methanol, and dried. Slow room temperature evaporation of solvent from the filtrate afforded orange-yellow crystals of **4**. Yield: 55 mg (1.57 mmol, 79%). Elemental anal. Calcd for C$_{21}$H$_{19}$NO$_4$: C, 72.19; H, 5.48; N, 4.01. Found: C, 72.10; H, 5.48; N, 3.80. IR (cm^{-1}): 3435 (ν OH), 3016/2955/2925 (ν CH), 1642 (ν C=O), 1628 (ν C=N), 1594/1545/1511 (ν C=C arom.), 1350 (δ OH), 1245 and 1109 (ν CO), 830 and 751 (δ CH).

Results and Discussion

The Schiff Base Nap-D,L-TyrOMe. The reaction between L-tyrosine methylester (TyrOMe) and *o*-hydroxynaphthaldehyde (nap) in methanol yielded yellow nap-TyrOMe. The bulk material clearly shows a CD effect and hence is racemic only in part. The crystals employed for the structure analysis were racemic. The Schiff base **4** crystallizes in the monoclinic space group $P2_1/n$ with 4 formula units per unit cell. Figure 1 shows the molecular structure and the arrangement of the molecules in the crystal lattice. Structure parameters are contained in Table 2. The molecule is present in its zwitterionic form with the proton from the phenol OH of the nap unit moved to the imine nitrogen, but the proton is still in intramolecular hydrogen-bonding contact with phenolate O4; d(N···O4) = 2.541 Å. The dihedral angle between the planes defined by the tyrosine and nap moieties is 55.1°.

The supramolecular arrangement (Figure 1, right) in the crystal comes about by hydrogen bonds between the Tyr-OH and the hydroxide of nap, d(O1···O4) = 2.601 Å, giving rise to zigzag chains with the molecules within each chain exclusively in the D- and L-configurations, respectively. The chains by themselves are interconnected by $\pi-\pi$ interactions between the naphthalene rings, with intermolecular C···C contacts between 3.33 and 3.55 Å.

Preparation and Structure of Complexes. The overall preparative scheme is provided in Scheme 1. The green complexes containing the tyrosine, serine, or threonine

Table 2. Selected Bond Lengths (pm) and Angles (deg) for **1a**−**c**, **2b**, and **4**

	1a/b	1c	4	2b
V−O1	1.578(2)	1.5944(16)		1.596(3)
V−O2	1.9825(19)	1.9773(16)		1.972(3)
V−O4	1.9101(19)	1.9043(15)		1.894(3)
V−O5	1.9996(2)	2.0077(16)		1.979(3)
V−N	2.019(2)	2.0341(18)		2.022(3)
O2−C9	1.296(3)	1.285(3)	1.3270(12)	
O3−C9	1.242(3)	1.241(3)	1.1864(13)	
N−C8	1.460(3)	1.467(3)	1.4386(11)	
N−C10	1.288(3)	1.291(3)	1.3033(12)	
O2−C1				1.302(4)
O3−C1				1.216(5)
N−C2				1.465(5)
N−C4				1.292(5)
O2−V−O4	145.91(9)	141.97(7)		141.97(7)
O2−V−N	79.31(8)	78.63(7)		78.63(7)
O4−V−N	87.19(3)	87.79(7)		87.79(7)
O5−V−N	144.03(9)	147.61(8)		147.61(8)

Scheme 1. Preparation of Complexes

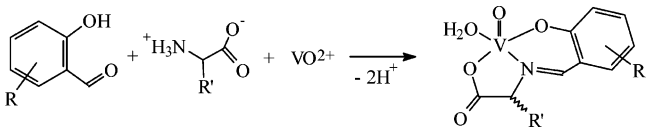

R =  ; R'= $CH_2C_6H_4OH$: **1a** (D), **1b** (L), CH_2OH: **2a**, $CH(CH_3)OH$: **3a**

R = 3-OCH_3; R'= $CH_2C_6H_4OH$: **1c**, CH_2OH: **2b**, $CH(CH_3)OH$: **3b**

moiety (**1a**, **1c**, **2**, **3**) were prepared in a one-pot reaction from the aldehyde, L-amino acid, and vanadyl sulfate in methanol/water or methanol under reflux in the presence of sodium acetate. The complexes crystallize with water or methanol of crystallization. For the threonine complexes **3a** and **3b**, additional purification of the raw product by recrystallization from THF/pentane was necessary. The reaction between $[VO(nap)_2]$ and L-tyrosine led to [(nap-D,L-Tyr)$VO(H_2O)$], from which crystals of [(nap-L-Tyr)$VO(H_2O)$] (**1b**) were picked and characterized by X-ray structure analysis.

The complexes attain the almost ideal tetragonal-pyramidal arrangement, with the tridentate ligand and a water molecule forming the tetragonal plane and the doubly bonded oxygen in the apex. Vanadium is 0.58−0.60 Å above the plane. The four molecules, for which molecular and crystal structures have been obtained, are depicted in Figure 2. For **1a** and **1b**, see also Scheme 2. For selected structure parameters, see Table 2. Bond lengths and angles are similar for all of the complexes and in the expected range.[22,27,28] When compared with the ligand **4**, there are changes in the intraligand bond lengths for groups taking part in coordination. The lengths of the C−O bonds of the carboxylate group, *d*(O2−C9) and *d*(O3−C9), become similar on coordination despite the fact that only one of the carboxylate oxygens coordinates. The difference in bond lengths between the imine nitrogen and its neighboring carbons, *d*(N−C8) and *d*(N−C10), increases as this nitrogen coordinates to vanadium.

There are extensive H-bonding net-works in the crystalline solids, involving the oxygen functions of the ligands, coordinated water, and solvent of crystallization, leading to, in addition to $\pi-\pi$ stacking interactions, complex supramolecular arrangements; cf. Figure 3 for **1a**, **1c**, and **2b**. In all of the crystal arrangements, the smallest subunit is a dimer, the monomeric units of which are connected by hydrogen bonds between the aqua ligand and the carboxylate. The vanadyl groups are oriented *anti*-orthogonal, caused by a screw axis in the case of the complex with nap-D-Tyr (**1a**) and nap-L-Tyr (**1b**), and a local inversion center in case of the van-Tyr complex **1c** and the van-Ser complex **2b**. In **1a**, two adjacent helices are interlaced (as indicated by the cutout in Figure 3, upper left) via methanol of crystallization, forming double-stranded chains. The dimers in **1c** and **2b** are interconnected by water of crystallization, implementing two-dimensional layers and further three-dimensional networks. Selected hydrogen-bond lengths and C···C distances between π-stacked aromatic moieties are collated in Table 3.

Of specific interest in the context of the model character for biological systems is the participation of the Tyr-OH and Ser-OH in hydrogen bonding. In the tyrosine-containing complexes **1a** and **1b**, the Tyr-OH (O6) is H-bonded to methanol of crystallization (O7), *d*(O6···O7) = 2.755 (**1a**) and 2.734 Å (**1b**). In **1c**, the Tyr-OH (O6) is linked to the uncoordinated carboxylate O (O3) of a neighboring molecule, *d*(O6···O3) = 2.764 Å. In the serine complex **2b**, one of the waters of crystallization is involved in H-bonding to Ser-OH, *d*(O6···O8) = 2.750 Å. Similar hydrogen-bonding interactions generated by the dangling OH groups of a tyrosine or serine moiety have been reported for the octahedral oxovanadium complexes.[21−24]

The unprecedented racemization of the amino acid constituents of the Schiff bases can be explained in analogy to the function of enzymes such as alanine racemase and aspartate aminotransferase, which contain the cofactor pyridoxal-5′-phosphate. This cofactor forms a Schiff base (ia in Scheme 3) with the amino acid, in tautomeric equilibrium with its zwitterionic form (iia). This is followed by a 1,3-hydrogen shift in a ketimine/aldimine ((ib)/(iib)) hybrid by intermediate deprotonation and reprotonation (accompanied by an inversion of configuration) of C_α.[29,30] In the natural system, deprotonation of the substrate (Su) is usually achieved by lysine; reprotonation is accomplished by tyrosine. In our systems, the base (B) for deprotonation may be provided by unreacted amino acid or by water.

One might expect to avoid racemization, if the preparation of the complexes is carried out in two successive steps, such as via the oxovanadium-bis(aldehyde) complex, followed by reaction with the amino acid, eq 1.

$$VO^{2+} + 2napH + 2Ac^- \rightarrow [VO(nap)_2] + 2HAc \quad (1a)$$

$$[VO(nap)_2] + HTyrH \rightarrow [VO(nap\text{-}Tyr)(H_2O)] + napH \quad (1b)$$

Although crystals of enantiopure [VO(nap-L-Tyr)(H_2O)], **1b**, have been obtained from L-tyrosine and $[VO(nap)_2]$, a

(29) Sun, S.; Toney, M. D. *Biochemistry* **1999**, *38*, 4058−4065.
(30) (a) Julin, D. A.; Wiesinger, H.; Toney, M. D.; Kirsch, J. F. *Biochemistry* **1989**, *28*, 3815−3821. (b) Goldberg, J. M.; Kirsch, J. F. *Biochemistry* **1996**, *35*, 5280−5291. (c) Esaki, N.; Yoshimura, T.; Soda, K.; Lim, Y. H. *ICR Annu. Rep.* **1998**, *5*, 46−47.

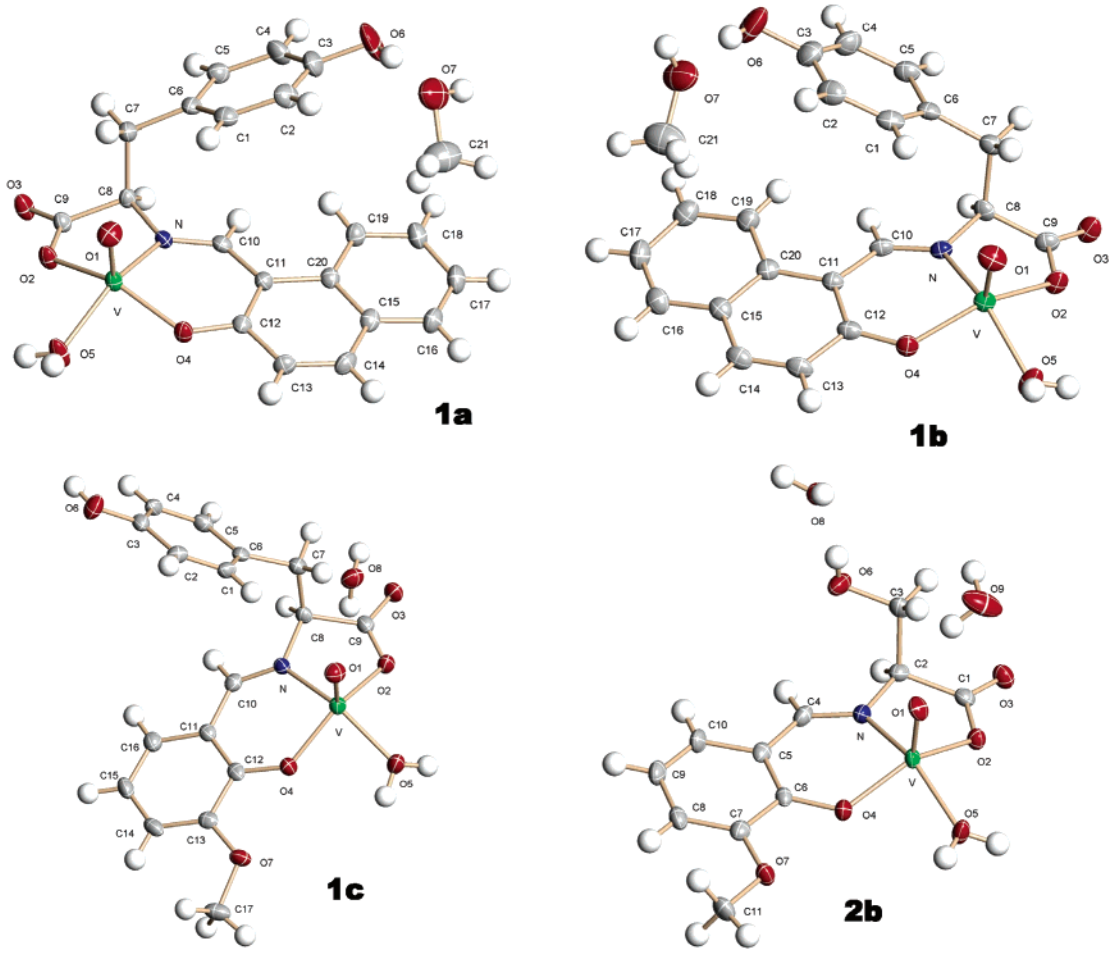

Figure 2. Molecular structures of [(nap-D-Tyr)VO(H_2O)]·MeOH (**1a**·MeOH), [(nap-L-Tyr)VO(H_2O)]·MeOH (**1b**·MeOH), [(van-D,L-Tyr)VO(H_2O)]·H_2O (**1c**·H_2O), and [(van-D,L-Ser)VO(H_2O)]·H_2O (**2b**·2H_2O).

Scheme 2. Schematic Drawings of [(nap-D-Tyr)VO(H_2O)] (**1a**, left) and [(nap-L-Tyr)VO(H_2O)] (**1b**, right)

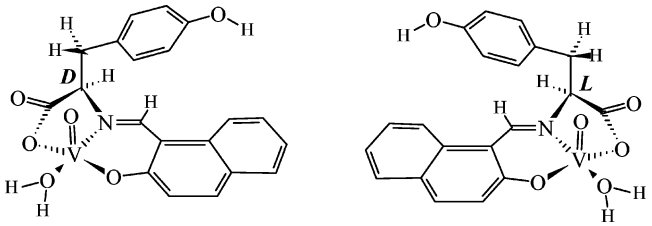

comparison of the CD spectra (Figure 4, left) of the bulk material of **1b** with that of **1a** ([VO(nap-D-Tyr)(H_2O)]), obtained in a one-pot reaction, clearly shows that partial racemization has occurred, even to a higher extent than in the reaction leading to crystals of **1a**. Apparently, [VO(nap)$_2$] does not react with tyrosine to a Schiff base complex in a template manner, but after dissociation of 2-oxy-naphthaldehyde from the vanadyl center and recoordination of the externally formed Schiff base.

The complexes exhibit UV−vis patterns characteristic of tetragonal-pyramidal VO^{2+} complexes with idealized C_{4v} symmetry. For these systems, three d−d transitions are anticipated, called band I (900−620 nm), band II (690−530 nm), and band III (480−330 nm), with band III commonly masked by CT transitions, particularly in the case of aromatic moieties as ligand constituents. Band I, corresponding to the $d_{xy}\rightarrow d_{xz},d_{yz}$ transition under local C_{4v} symmetry, can be split in IA and IB if the degeneracy of the d_{xz},d_{yz} set is lifted. The spectra of our compounds show a broad band I (unresolved with respect to components A and B) and band II for the tyrosine and threonine complexes, whereas band III and band II in the serine complexes are disguised by strong CT bands. A series of typical spectra is shown in Figure 4, right, and data are listed in Table 4.

The complexes are stable under aerobic conditions in solvents such as water, methanol and DMF. Cyclovoltammetry (in water and DMF) revealed irreversible oxidation and reduction steps only. As expected for d^1 systems, the complexes are paramagnetic, with a magnetic moment of 1.7(2) BM in solution (determined by the Evans method). Correspondingly, they are EPR active, providing axial anisotropic EPR patterns. The lack of resolved rhombic distortions[31] is in accord with the almost undistorted tetragonal structure found in the solid state and the lacking splitting of band I in the UV−vis spectra of solutions of the compounds. The similarity between the EPR parameters of the threonine derivatives with those of the tyrosine and serine derivatives supports the assumption that the threonine complex **3**, for which single-crystal structure data have not

(31) Garribba, E.; Micera, G.; Panzanelli, A.; Sanna, D. *Inorg. Chem.* **2003**, *42*, 3981−3987.

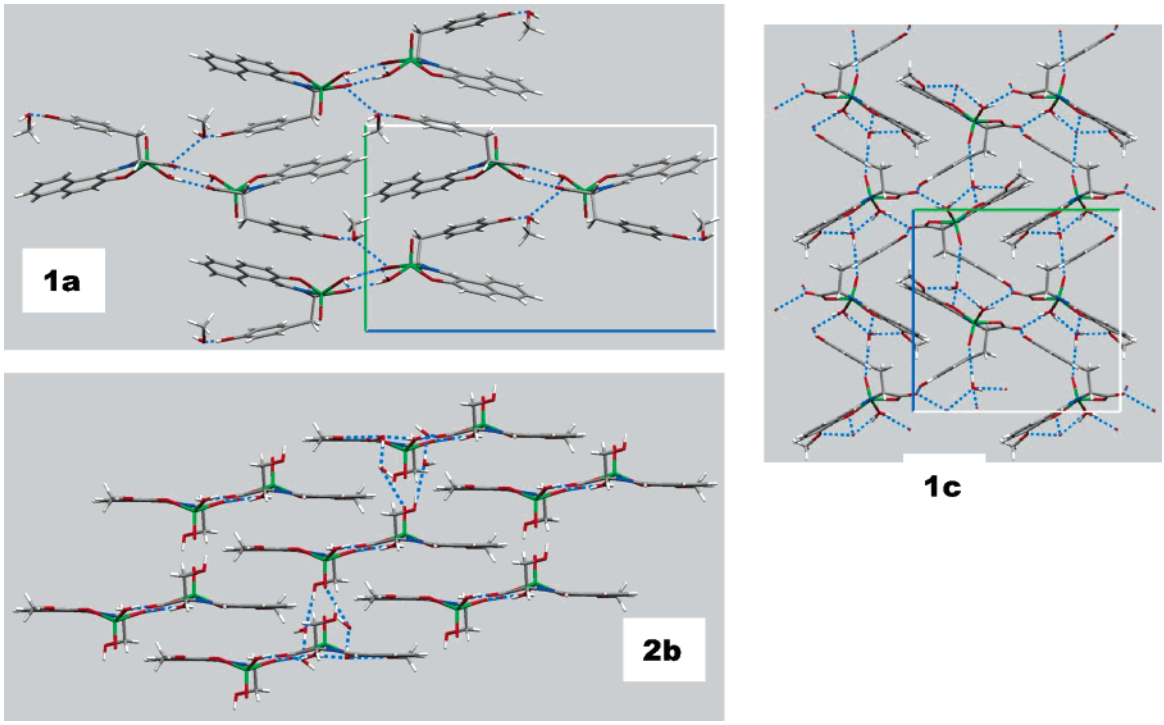

Figure 3. Supramolecular arrangements for the complexes [(nap-D-Tyr)VO(H_2O)]·MeOH (**1a**·MeOH), [(van-D,L-Tyr)VO(H_2O)]·H_2O (**1c**·H_2O), and [(van-D,L-Ser)VO(H_2O)]·H_2O (**2b**·2H_2O), viewed along the *a* axis (**1a** and **1c**) and the *c* axis (**2b**).

Table 3. Selected Distances (Å) between Hydrogen-Bridged Atoms and $\pi-\pi$ Stacked Moieties[a]

1a	1b	1c	2b
O3···O5′ 2.66, 2.71 (carboxylate···aqua)	O3···O5′ 2.66, 2.70 (carboxylate···aqua)	O3···O6′ 2.75 (carboxylate···TyrOH)	O2···O5′ 2.67 (carboxylate···aqua)
O2···O7′ 3.02 (carboxylate···MeOH)	O2···O7′ 3.02 (carboxylate···MeOH)		O3···O9′ 2.80 (carboxylate···water)
O6···O7 2.76 (TyrOH···MeOH)	O6···O7 2.73 (TyrOH···MeOH)	O8···O1/O4/O5/O7 2.81−3.03 (water···cf. Figure 2)	O6···O8 2.75 (SerOH···water)
Tyr···nap (closest C···C) average 3.49	Tyr···nap (closest C···C) average 3.49	Tyr···nap (closest C···C) average 3.44	C7···C7′ 3.50

[a] A primed atom indicates a contact to a neighboring molecule.

Scheme 3. Mechanism for Racemization of a Schiff Base Containing an *o*-Phenol Moiety

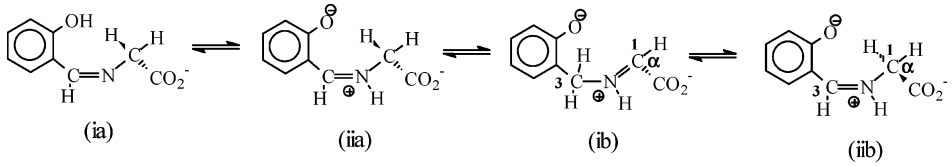

coupled with : $B + SuH \rightleftharpoons (BH)^+ + Su^-$ (*Su* = substrate, B = base)

Table 4. UV−Vis Absorptions[a]

	band I	band II	CT bands
1a (methanol)	712 (24)	529 (66)	398 (6510), 326 (9205)
1c (water)	753 (21)	535 (38)	390 (2310), 288 (10270)
2a (water)	794 (27)		399 (4920), 326 (8370)
2b (water)	606 (43)		336 (2650), 246 (10185)
3a (water)	702 (45)	519 (81)	387 (4895), 326 (3410)
3b (water)	791 (16)	526 (34)	387 (2050), ca. 290 (ca. 9000)

[a] Wavelengths λ in nanometers, absorption coefficient ϵ (in parentheses) in L mol^{-1} cm^{-1}

been obtained, is structurally equivalent to complexes **1** and **2**. Experimental EPR, isotropic and anisotropic *g* factors, and hyperfine coupling constants *A* are given in Table 5. The experimental parallel component of *A*, A_z, is in good agreement with the calculated $A_z = 168 \times 10^{-4}$ cm^{-1} on the basis of the additive contributions[32] of the four equatorial ligands: H_2O, 45.7;[33] N(Schiff base), 41.6;[34] carboxylate, 42.1;[35] and phenolate, 38.6.[33] The slight deviation of the calculated from the experimental value may have its root in the uncertainty of the contribution of the N(Schiff base)

(32) (a) Tasiopoulos, A. J.; Deligiannakis, Y. G.; Woollins, J. D.; Slawin, A. M. Z.; Kabanos, T. A. *Chem. Commun.* **1998**, 569−570. (b) Cornman, C. R.; Zovinka, E. P.; Boyajian, Y. D.; Geiser-Bush, K. M.; Boyle, P. D.; Singh, P. *Inorg. Chem.* **1995**, *34*, 4213−4219.
(33) Smith, T. S., II; LoBrutto, R.; Pecoraro, V. L. *Coord. Chem. Rev.* **2002**, *228*, 1−18.
(34) Garribba, E.; Lodyga-Chruscinska, E.; Micera, G.; Panzanelli, A.; Sanna, D. *Eur. J. Inorg. Chem.* **2005**, 1369−1382.
(35) Jakusch, T.; Buglyó, P.; Tomaz, A. I.; Costa Pessoa, J.; Kiss, T. *Inorg. Chim. Acta* **2003**, *339*, 119−128.

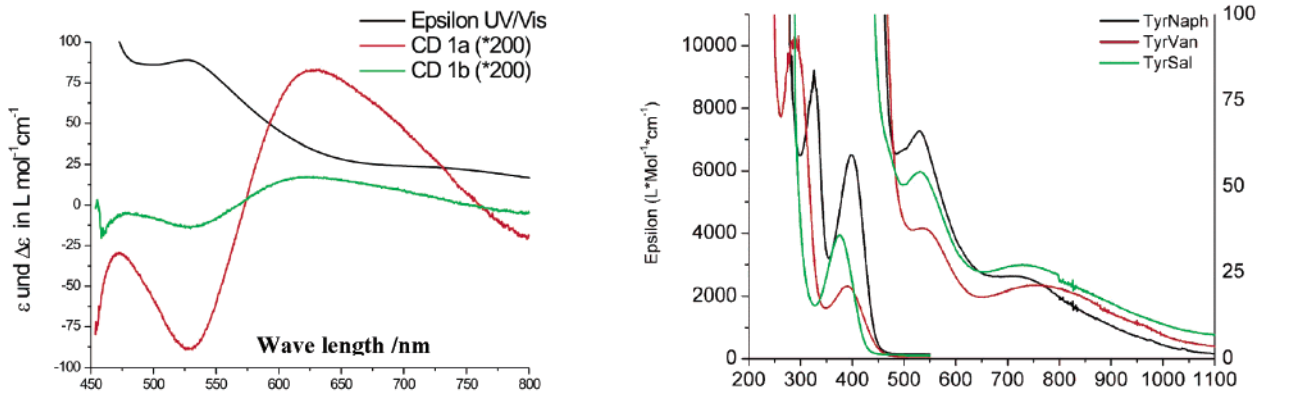

Figure 4. Left: CD spectra (in methanol) of the bulk materials of the [VO(nap-Tyr)(H_2O)] complexes **1a** (red) and **1b** (green). The ϵ scale has been extended by a factor of 200 with respect to that of the UV−vis absorption (black). Both **1a** and **1b** exhibit a CD effect due to the presence of excess L-enantiomer. Right: UV−vis spectra of three oxovanadium−Schiff base complexes (in methanol or (TyrVan) water) containing tyrosine moieties. All spectra have been obtained at ambient temperature.

Table 5. Experimental EPR Parameters

	g_{iso}	$A_{iso}{}^a$	g_{xy}	g_z	$A_{xy}{}^a$	$A_z{}^a$
1a	1.9915	93.0	1.985	1.951	63	170.5
1c	1.991	93.0	1.982	1.951	61	170
2a	1.9917	93.0	1.9835	1.950	62	170
2b	1.9877	91.3	1.982	1.949	62	171
3a	1.991	93.0	1.983	1.950	61	170
3b	1.991	92.5	1.984	1.951	62	170

[a] In units of 1×10^{-4} cm^{-1}.

function, which varies, according to the orientation of the Schiff base with respect to the tetragonal plane, between 38.1 and 43.7 $\times$ 10^{-4} cm^{-1}.[34] The parameters are further in agreement with those of oxovanadium(IV) Schiff base complexes containing amino acid constituents without functionalized side chains.[28]

Conclusion

Schiff bases of the type employed here contain an ON(X)O donor set (X is the O(H) functionality of the amino acid component) and thus can, in principle, model the binding ability of N_{amide}(X) or/and O_{amide}(X) function(s) within the protein to metal cations and oxometalates. The coordinating functions available in the Schiff bases, acting here as tridentate ligands, provide stable complexes. The photoinduced deactivation of, for example, SR ATPase[4] and myosine subfragment S1[1,2] in the presence of vanadate, and the photoinduced activation of serine sulfhydrase,[6] again catalyzed by vanadate, go along with a redox interaction between vanadate (which is reduced to vanadyl) and active site serine (oxidation to formylglycine) or cysteine (oxidation to serine). Active center serine has further been shown to possibly play a role in the oxidation of bromide to hypobromous acid by vanadate-dependent peroxidases.[36] For tyrosine, redox activity in proteins is well-established. With dipeptides such as glycyl-tyrosine, coordination to vanadate via the terminal amino and carboxylate functions plus the deprotonated amide takes place along with reduction of vanadate to vanadyl.[19] VO^{2+}, which can also form by cytosolic reduction of vanadate by, e.g., glutathion,[37] coordinates to proteins more efficiently and more directly (i.e., through covalent bonds) than does vanadate. With the present study, we show that complex formation of VO^{2+} with ligand functions providing a set of donors suitable for the formation of bicyclic chelate motifs is favored with respect to coordination to phenolate (in the case of tyrosine) or alcoholate (in the cases of serine and threonine). The dangling nature of the Ser-OH has previously been established for the dinuclear, anionic oxovanadium(IV,V) complex $[V_2O_3$(sal-D,L-Ser)$_2]^-$.[22] The OH functionalities are, however, involved in hydrogen bonding. Similarly, VO^{2+}, when formed from vanadate by (light-induced) redox interaction with amino acid side chains such as serine and cysteine, will preferentially coordinate to the backbone amide plus carboxylate and nitrogen donors such as provided by histidine.[38] Additionally, interlinkages through hydrogen bonds, as modeled by the supramolecular networks of our vanadyl−Schiff base complexes, should be formed. An additional aspect of potential involvement of vanadyl ions in biological systems is the racemization of the OH-functional amino acid as a constituent of a coordinating protein moiety, modeled here by the (partial) racemization of the L-amino acid in the course of its integration into the coordination sphere.

Acknowledgment. This work was supported by a grant from the Deutsche Forschungsgemeinschaft.

IC0602953

(36) Christmann, U.; Dau, H.; Haumann, M.; Kiss, E.; Liebisch, P.; Rehder, D.; Santoni, G.; Schulzke, C. *Dalton Trans.* **2004**, 2534−2540.
(37) Li, J.; Elgberg, G.; Crans, D. C.; Shechter, Y. *Biochemistry* **1996**, *35*, 8314−8318.
(38) Schmidt, H.; Andersson, I.; Rehder, D.; Pettersson, L. *Chem.−Eur. J.* **2001**, *7*, 251−257.